AGU PUBLICATIONS

JGR

Journal of Geophysical Research: Earth Surface

RESEARCH ARTICLE
10.1002/2016JF003932

Key Points:
- A physical model is presented that predicts the spectral albedo and melt impact of algal blooms on snow for the first time
- "Bioalbedo" is shown to impact the melt rate of snow, and associated indirect feedback are shown to be important
- Spectral "signatures" are identified that could be used to detect life in snow and ice from remotely sensed spectral reflectance data

Supporting Information:
- Supporting Information S1

Correspondence to:
J. M. Cook,
joe.cook@sheffield.ac.uk

Citation:
Cook, J. M., A. J. Hodson, A. J. Taggart, S. H. Mernild, and M. Tranter (2017), A predictive model for the spectral "bioalbedo" of snow, *J. Geophys. Res. Earth Surf.*, *122*, 434–454, doi:10.1002/2016JF003932.

Received 22 APR 2016
Accepted 13 DEC 2016
Accepted article online 11 JAN 2017
Published online 31 JAN 2017

A predictive model for the spectral "bioalbedo" of snow

J. M. Cook[1,2], A. J. Hodson[1,3], A. J. Taggart[1], S. H. Mernild[4,5,6], and M. Tranter[7]

[1]Department of Geography, University of Sheffield, Sheffield, UK, [2]College of Life and Natural Sciences, University of Derby, Derby, UK, [3]Arctic Geology, University Centre in Svalbard, Longyearbyen, Norway, [4]Faculty of Engineering and Science, Sogn og Fjordane University College, Sogndal, Norway, [5]Antarctic and Subantarctic Program, Universidad de Magallanes, Punta Arenas, Chile, [6]Nansen Environmental and Remote Sensing Centre, Bergen, Norway, [7]Bristol Glaciology Centre, School of Geographical Sciences, University of Bristol, Bristol, UK

Abstract We present the first physical model for the spectral "bioalbedo" of snow, which predicts the spectral reflectance of snowpacks contaminated with variable concentrations of red snow algae with varying diameters and pigment concentrations and then estimates the effect of the algae on snowmelt. The biooptical model estimates the absorption coefficient of individual cells; a radiative transfer scheme calculates the spectral reflectance of snow contaminated with algal cells, which is then convolved with incoming spectral irradiance to provide albedo. Albedo is then used to drive a point-surface energy balance model to calculate snowpack melt rate. The model is used to investigate the sensitivity of snow to algal biomass and pigmentation, including subsurface algal blooms. The model is then used to recreate real spectral albedo data from the High Sierra (CA, USA) and broadband albedo data from Mittivakkat Gletscher (SE Greenland). Finally, spectral "signatures" are identified that could be used to identify biology in snow and ice from remotely sensed spectral reflectance data. Our simulations not only indicate that algal blooms can influence snowpack albedo and melt rate but also highlight that "indirect" feedback related to their presence are a key uncertainty that must be investigated.

1. Introduction

Snow has a more variable albedo than any other surface on Earth, ranging from as high as 0.98 for fresh, clean snow to 0.3 in the visible wave band for snow heavily laden with light-absorbing impurities [*Flanner and Zender*, 2006; *Painter et al*., 2013]. This variability exerts an important influence on global climate via the snow-albedo feedback [*Budyko*, 1969]. The amount of incident solar radiation absorbed by snow and available for driving snowmelt is very sensitive to changes in the optical properties of snow. Grain size and impurity concentration are the primary inherent characteristics that evolve seasonally and determine the optical properties and albedo of snow [e.g., *Wiscombe and Warren*, 1980; *Warren*, 1982; *Aoki et al*., 2003; *Flanner and Zender*, 2006; *Painter et al*., 2001]. Many previous studies have quantified the albedo effect of inorganic impurities, such as mineral dust and black carbon (BC), on snow [*Clarke and Noone*, 1985; *Flanner et al*., 2007; *Brandt et al*., 2011; *Hadley and Kirchstetter*, 2012]. The effect of biological impurities ("bioalbedo") has yet to be isolated from other impurities and snow grain metamorphosis effects despite being recognized as potentially important for snow spectral albedo [*Painter et al*., 2001; *Benning et al*., 2014]. These effects have yet to be incorporated into a predictive radiative transfer model (RTM). This means that we cannot properly characterize snow albedo in general climate models because an appropriate, physically based understanding of the sensitivity of snow albedo to the full suite of biotic, biogenic, and abiotic impurities is lacking.

Cold-adapted or cold-tolerant algae are commonly found in high-latitude snow and may be important test organisms for research into cold and UV tolerance [*Remias et al*., 2010]. The most common snow alga is often reported to be *Chlamydomonas nivalis*, which has been identified in snow in Antarctica [*Edwards et al*., 2004], Svalbard [*Stibal et al*., 2007], Iceland [*Lutz et al*., 2015], Greenland [*Lutz et al*., 2014), the Russian Arctic [*Hisakawa et al*., 2015], and the Alps [*Remias et al*., 2010]. However, many snow algae share morphological traits which can vary dramatically throughout their life cycles, making accurate identification difficult. Several molecular studies indicate that snow algal communities are often dominated by the species *Chloromonas* or *Chlamydomonadaceae* [*Hoham and Duval*, 2001; *Leya*, 2004]. To avoid confusion, we simply refer to "red snow algae" in this paper, and note that we mean red colored rather than taxonomically red (i.e., *Rhodophyta*). Red snow algae are known to produce photoprotective pigments in response to exposure to UV

[*Remias et al*., 2010], which has been suggested to enhance its darkening effect on the ice surface. Darker ice melts more rapidly due to the efficient absorption of solar energy.

A physically based approach is appropriate in the development of predictive models, because it is very difficult to separate algal cells from the other particulates and snow physical properties which impact on albedo. Difficulties in culturing these algae also make it challenging to measure their spectral reflectance independent of snow properties. It has been suggested that algae can cause snow albedo to drop to values as low as 0.4 [*Hisakawa et al*., 2015]; however, no studies to date have measured the albedo-reducing effect of algae alone, independent of snow physical properties and additional impurities. Care must be taken to consider the impact of impurities in the context of changing snow physical properties, given that old waterlogged snow may have an albedo as low as 0.5, compared to a typical fresh, clean snow albedo of 0.7–0.9 (see review by *Gardner and Sharp* [2010]). Furthermore, there is widespread ambiguity in the measurement and reporting of reflectance values [*Schaepman-Strubb et al*., 2006] that can make interpretation and interstudy comparison of empirical data difficult or impossible. In this paper, we follow the reflectance terminology of *Nicodemus et al*. [1977] for clarity and consistency with remote sensing literature.

A fully predictive model for the albedo of snow will necessarily include both snow physics (which are well served by existing RTMs, including Two-streAm Radiative TransfEr in Snow (TARTES) [*Libois et al*., 2013] and Snow, Ice, and Aerosol Radiation [*Flanner et al*., 2007] as well as snow evolution models such as CROCUS (an energy and mass evolution model forced by meteorological data) [*Brun et al*., 1989]) and several impurity types, including mineral dusts, BC, and algal cells. The optical properties of each impurity must be known individually in order for such a model to be developed. Predicted spectral reflectance will facilitate deeper analysis of remotely sensed spectra from orbital and suborbital platforms, allowing identification and quantification of the impurities and deriving glaciological and ecological information about the snow or ice mass.

A model has been developed that combines physical modeling of single-cell biooptics with a two-stream radiative transfer model and point-surface energy balance model to investigate the sensitivity of snow surfaces to blooms of snow algae. The model consists of a fully predictive biooptical model adapted from *Pottier et al*.'s [2005] model of light attenuation in photobioreactors, a radiative transfer model for predicting the albedo of multiple layers of snow (TARTES), and a point-surface energy balance model [*Brock and Arnold*, 2000] for predicting melt. The model predicts changes in reflectance, convolves this with incoming spectral irradiance to provide albedo, and then uses an energy balance scheme to predict melt rate with variations in algal biomass, cell size, and pigmentation.

Here we describe a sensitivity study for snow surfaces populated with red snow algae. We held constant the physical properties of the snow and the meteorological (including irradiance) conditions in order to isolate the sensitivity of snow surfaces to algal blooms (although we note that in real systems there are likely feedback between biological activity and snow grain evolution, as discussed later). We calculated the bihemispheric reflectance factor (BHR) of various snowpacks, individually altering the concentration of each pigment in the cells, the cell size, and the biomass loading. Then, a range of bloom scenarios were simulated, varying values for cell size, pigment mass fractions, and biomass concentration. Incoming solar radiation data were simulated using NASA's Coupled Ocean-Atmosphere Radiative Transfer (COART) model and convolved with the BHR to provide spectral and broadband albedos (α_λ and α). Real blooms observed by *Painter et al.* [2001] and *Lutz et al.* [2014] were forward modeled to compare our simulations to empirical measurements and demonstrate the utility of our model for both forward and inverse modeling of snowpack reflectance. Broadband albedo was then fed into the energy balance model. We also quantify for the first time how shallow subsurface blooms could influence the albedo of the snowpack. Finally, we draw upon our spectral albedo simulations to discuss the potential for algal life detection from satellite remote sensing.

2. Model Structure

To determine the relevant optical properties of algal cells for radiative transfer modeling, the complex refractive index of the algal cells must first be known. The complex index of refraction consists of a real part (n), representing scattering, and an imaginary part (ik_λ, where $i=\sqrt{-1}$ and k_λ = absorption coefficient) representing absorption.

$$m = n \mp ik_\lambda \tag{1}$$

The real part is approximately wavelength independent [*Dauchet et al.*, 2015], whereas the imaginary part varies across the electromagnetic spectrum. The real part of the refractive index can be determined experimentally by measuring the absorption through a cell at a nonabsorbing wavelength (commonly 820 nm for *Chlamydomonas reinhardii*). Here we assume that the real part of the refractive index for our snow algae is equal to that of *C. reinhardii*, because this species is a good analogue for *C. nivalis*, and *Dauchet et al.* [2015] showed this value to be near constant between microbial cells. The imaginary part of the refractive index, k_λ, was predicted using the following equations, adapted from *Pottier et al.* [2005].

$$k_\lambda = \frac{\lambda}{4\pi} \rho_i \frac{1 - x_w}{x_w} \sum_{i=1}^{N} Ea_i(\lambda) \,.\, w_i \tag{2}$$

where

$$x_w = 1 - \frac{C_x}{N_p} \frac{1}{V_{32}} \frac{1}{\rho_i} \tag{3}$$

where C_x = dry mass concentration (kg m^{-3}), N = number of pigments, N_p = number particle density (m^{-3}), and V_{32} = mean efficient volume for the particle (m^3), and all other definitions are in Table 1. To obtain k_λ from these equations, the in vivo spectral mass absorption coefficient (Ea_λ) for each pigment (i) must be known. Little information regarding these data are available in the literature; however, *Bidigare et al.* [1990] provide Ea_λ for the major algal pigments (Figure 1). We define primary carotenoids as those directly involved in photosynthesis and secondary carotenoids as those with other functions, such as photoprotection. We assume that these Ea_λ values are appropriate for our snow algae but caution that more research is required into the variations between in vitro and in vivo absorption by various pigments in different organisms (for example, due to the formation of complexes and obscuration by organelles). This model also assumes that the pigments are the only absorbing components in each cell. The water fraction (x_w) and density (ρ_i) of the cells are assumed to be a constant (0.8 and 1400 kg m^{-3}, respectively) for microalgal cells, as justified by *Dauchet et al.* [2015].

The assumption that algal cells are spherical and homogeneous facilitates the use of Lorenz-Mie theory for calculating the absorption (Q_{abs}), scattering (Q_{sca}), extinction (Q_{ext}), and backscattering (Q_{bb}) efficiency factors from k_λ and cell diameter for the algal cells. However, the diameter alone is insufficient to describe photon interactions with cells of different sizes. More appropriate is a measure that relates cell size to the wavelength of light propagating through the medium. This term is χ and is defined in equation (4).

$$\chi = \pi d_p / \lambda \tag{4}$$

Since attenuation is the result of scattering and absorption, the efficiency factors Q_{ext} and Q_{sca} are related to Q_{abs} by the relationship

$$Q_{ext} = Q_{sca} + Q_{abs} \tag{5}$$

This is useful information for comparing the optical properties of individual algal cells under different growth and pigmentation condition and may prove useful for remote sensing of biological impurities in the cryosphere. However, for the sake of computational simplicity we do not employ a full Lorenz-Mie computation in our radiative transfer modeling. Instead, we assign values to the real and imaginary parts of the complex refractive index according to our biooptical model and assume that cells impact the absorption cross section but not the scattering cross section of the snow, justified by the low cell content in the snow and the negligible influence of impurities on snowpack scattering [e.g., *Zatko et al.*, 2013; *Stamnes and Stamnes*, 2016]. This assumption is built in to the published version of TARTES for all impurities (see TARTES scientific documentation) and was also implicit in *Aoki et al.*'s [2013] model for ice and snow surface albedo which varied the refractive index in a mineral-dust model to simulate algal blooms.

The RTM TARTES [*Libois et al.*, 2013] predicts the albedo of a snowpack given concentrations and absorption cross sections of impurities and snow physical properties. This is achieved using *Kokhanovsky and Zege*'s [2004] equations for weakly absorbing media, and the radiative transfer calculations are solved using the Delta-Eddington approximation, which involves summing the two-stream

Table 1. Parameters Required for Modeling

Symbol	Parameter	Model	Constant or Variable?	Value	Source
BHR	Bihemispheric reflectance factor	RTM	Variable	0–1	Predicted by RTM
α_λ	Albedo (spectral; defined as BHR convolved with incoming spectral solar irradiance)	RTM, EB	Variable	0–1	Predicted by RTM
α_{vis}	Albedo, integrated across the visible wave band (400–700 nm)	RTM, EB	Variable	0–1	Predicted by RTM
α_{BB}	Broadband albedo, integrated between 400 and 2200 nm	RTM, EB	Variable	0–1	Predicted by RTM
$Ea_{\lambda,i}$	In vivo spectral absorption coefficient for each pigment ($m^2\ mg^{-1}$)	Biooptic	Constant	0–0.07	*Bidigare et al.* [1990] and *Li et al.* [2012]
ρ_i	Density of cellular dry material ($kg\ m^{-3}$)	Biooptic	Constant	1400	*Dauchet et al.* [2015]
w_i	Mass fraction of each pigment (percent total cellular dry mass)	Biooptic	Variable	0.0001–0.05	*Remias et al.* [2010] and *Lutz et al.* [2014]
x_w	Water fraction in cell (vol %)	Biooptic	Constant	0.78	*Dauchet et al.* [2015]
n_m	Real part of refractive index for snow	Biooptic	Constant	1.3	*Warren and Brandt* [2008]
n	Real part of refractive index for algal cells	Biooptic	Constant	1.5	*Dauchet et al.* [2015]
k_λ	Imaginary part of refractive index (i.e., absorption coefficient)	Biooptic, RTM	Variable	Modeled	na
z_s	Thickness of each snow layer, s (m)	RTM	Variable	1–3 for top (algal) layer	*Lutz et al.* [2014]
SSA	Snow SSA ($m^2\ kg^{-1}$)	RTM	Variable	0.1–30	*Libois et al.* [2013] and *Gallet et al.* [2014]
D	Snow density ($kg\ m^{-3)}$	RTM	Variable	250–950	*Libois et al.* [2013] and *Gallet et al.* [2014]
I	Irradiance	RTM	Variable	Modeled	COART[a]
Z	Surface roughness (m)	EB	Constant	0.001	PROMICE[b]
SWR	Shortwave flux ($W\ m^{-2}$)	EB	Constant	Time series	PROMICE[b]
LWR	Longwave flux ($W\ m^{-2}$)	EB	Constant	Time series	PROMICE[b]
T_a	Air temperature (°C)	EB	Constant	Time series	PROMICE[b]
V_p	Vapor pressure (Pa)	EB	Constant	Time series	Calculated from PROMICE[b] using *Tetons* [1930] method
WS	Wind speed ($m\ s^{-1}$)	EB	Constant	Time series	PROMICE[b]
Lat	Latitude (degrees)	EB	Constant	7285631°N	PROMICE[b]
Lon	Longitude (degrees)	EB	Constant	0551705°E	PROMICE[b]
RH	Relative humidity (%)	EB	Constant	Time series	PROMICE[b]
Slope	Slope (degrees)	EB	Constant	5°	PROMICE[b]
Elevation	Elevation (m)	EB	Constant	Site specific	*Lutz et al.* [2014]

[a]COART refers to the NASA Coupled Ocean-Atmosphere Radiative Transfer Model, available at http://cloudsgate2.larc.nasa.gov/jin/coart.html [*Jin et al.*, 2006].
[b]PROMICE refers to the PROMICE automatic weather station MIT (www.promice.org).

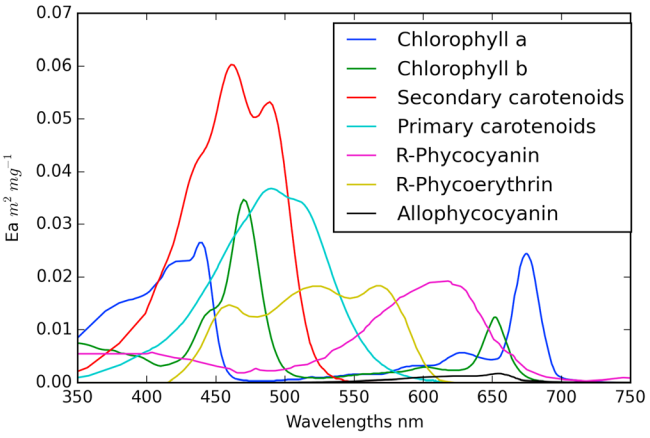

Figure 1. In vivo absorption coefficients for algal pigments; drawn from data in *Bigidare et al.* [1990] and *Li et al.* [2012].

fluxes in each vertical layer. TARTES assumes that the snowpack can be accurately represented as a collection of spheres with equal specific surface area (SSA) to the real nonspherical grains. SSA can be measured via infrared reflection spectra [*Gallet et al.*, 2009] or calculated from snow density (ρ_{ice}) and effective grain radius (r_{eff}; equation (6)):

$$SSA = \frac{3}{\rho_{ice} r_{eff}} \quad (6)$$

This simplification allows radiative fluxes to be calculated with error <5% [*Grenfell and Warren*, 1999; *Neshyba et al.*, 2003; *Grenfell et al.*, 2005], but it is not useful for

calculating directional reflectance [*Painter and Dozier*, 2004]. TARTES represents the snowpack as a series of layers which are horizontally homogenous and characterized by SSA, density, and impurities. Impurities are described by distinct classes that contain information regarding their complex refractive index and density. Black carbon (BC) and humic-like substances are included in the published version of TARTES, using RI (refractive index) and density data from *Bond and Bergstrom* [2006] and *Hoffer et al.* [2006], respectively. For detailed discussion of the treatment of the snow crystals in the RTM, we point to the TARTES documentation (http://lgge.osug.fr/~picard/tartes/) and *Libois et al.* [2013] along with wider discussion of radiative transfer in snow grains in *Warren* [1982] and an excellent review by *Gardner and Sharp* [2010].

We defined a new class of impurity ("algae") in TARTES and also defined the physical properties of the snowpack, including specific surface area (SSA), density, and thickness of each snow layer (with the bottom layer being semiinfinite in the vertical dimension). Algal cells and other impurities are assumed to be externally mixed; i.e., they only occur outside of snow grains. We adapted TARTES to predict the spectral BHR of the snowpack with various bloom intensities and with a range of biooptical properties. Albedo is distinct from BHR in that it depends not only upon the inherent optical properties of the surface but also the characteristics of the incoming light (illumination angle, spectral distribution, and cloud and atmospheric interference). We therefore convolved BHR with spectral at-surface solar irradiance predicted by the COART model for specific sites and dates, providing both spectral and spectrally integrated albedo values (equations (7) and (8)):

$$\alpha_\lambda = \frac{\mathrm{BHR}_\lambda \times I_\lambda}{I_\lambda} \tag{7}$$

$$\alpha = \frac{\int \mathrm{BHR}_\lambda \times I_\lambda}{\int I_\lambda} \tag{8}$$

The integrated albedo can then be used to drive *Brock and Arnold*'s [2000] point-surface energy balance model, which returns melt in millimeter water equivalent. This model estimates the surface energy balance for melting snow and therefore ignores heat conduction into the snowpack and assumes that rainfall is a negligible heat transfer process compared to shortwave radiation flux and turbulent transfer of latent and sensible heat. The model is site specific and driven by hourly meteorological data including incoming shortwave radiation, air temperature, vapor pressure, and wind speed, along with the Julian day and hour, site latitude and longitude, slope, aspect, elevation, temperature lapse rate, surface broadband albedo, and aerodynamic roughness length. The melt is calculated as the residual of the equation

$$\mathrm{MLT} = \mathrm{SWR} + \mathrm{LWR} + \mathrm{SHF} + \mathrm{LHF} \tag{9}$$

where MLT = melt, SWR = shortwave radiation flux, LWR = longwave radiation flux, SHF = sensible heat flux, and LHF = longwave radiation flux. Our model combination hence simulates the melt impact of red algae on snow. Depending upon data availability and user preference, the model can output BHR, spectral albedo, broadband albedo, or melt rate.

3. Results

We first used Lorenz-Mie theory to examine variations in optical properties of individual cells of varying size and pigmentation. Then, we studied the impact of cell optics at the population level on snowpack albedo. We determined the sensitivity of snowpacks to algal blooms by holding the snow physical and meteorological variables constant and systematically varying the optical properties of the algal cells and the biomass concentration in the snow. We then tested the ability of the model to recreate field data by simulating blooms measured by *Painter et al.* [2001] (spectral) and *Lutz et al.* [2014] (broadband). For the latter, where meteorological data are available, we use predicted broadband albedo to drive melt modeling. We then model the impact of subsurface blooms on snowpack albedo and melt rates and finally discuss potential spectral biosignatures that might facilitate remote sensing of snow algae.

3.1. Optical Properties of Red Snow Algae

3.1.1. Lorenz-Mie Efficiency Factors

Q_{bb} is an important parameter for the remote sensing of algal cells in the ocean [e.g., *Stramski and Kiefer*, 1991; *Stramski and Morel*, 1990; *Stramski et al.*, 2004] and should also be examined as a potential tool for remote sensing of algae in snow. Backscattering is dependent upon wavelength, cell size, and refractive

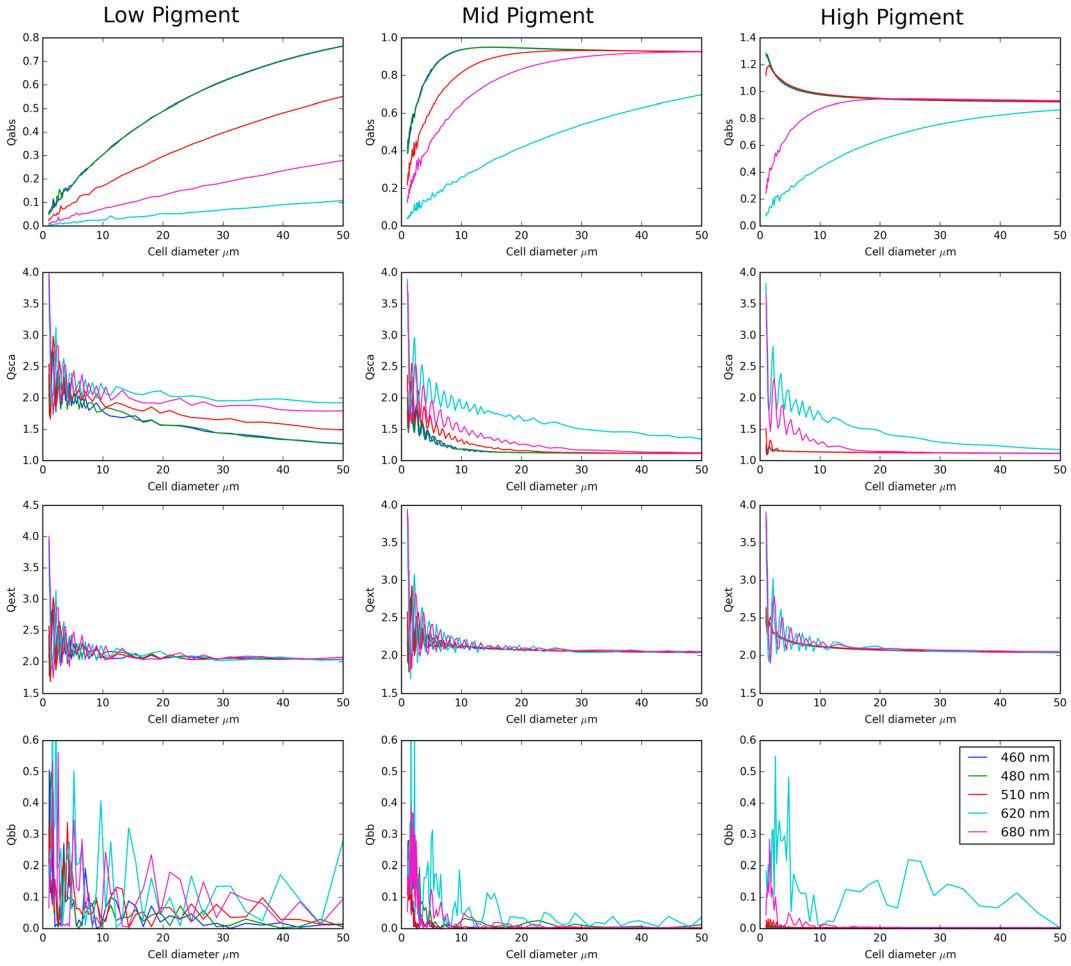

Figure 2. Q_{abs}, Q_{sca}, Q_{ext}, and Q_{bb} with increasing cell diameter for five wavelengths. The legend in the bottom right figure is common to all subplots.

index (the imaginary part of which varies according to cell pigmentation). We used Lorenz-Mie theory to calculate the absorption (Q_{abs}), scattering (Q_{sca}), extinction (Q_{ext}), and backscattering (Q_{bb}) efficiency factors for snow algal cells of varying size (between 1 and 50 μm) for a selection of wavelengths (Figure 2). The wavelengths were selected to enable comparison with other published work on algae in other environments and bioreactors. The experiment was repeated for three pigment scenarios: low, medium, and high (Table 2). For all wavelengths in the low- and medium-pigment scenarios, Q_{abs} increases with wavelength before plateauing at ~0.9. This is unsurprising since larger cells represent a greater volume of material available to absorb incident radiation. The shape of the curve varies according to wavelength, with longer wavelengths generally having shallower curves and plateauing at larger cell diameters. However, this was not the case for 620 nm. This is readily explained by the spectral absorption coefficient of the cell, which is dominated by secondary carotenoids (400–550 nm) and chlorophylls (350–450 and 660–690). This means that 620 nm is close to the absorption minimum for the cell, and consequently, Q_{abs} is lower at that wavelength. Similarly, Q_{sca} generally decreases with increasing cell size (which is unsurprising since smaller cells provide more opportunity for scattering at air-cell interfaces) but is greatest at 620 nm. This is because Q_{sca} is calculated relative to absorption, which is at its minimum at 620 nm. For the high-pigment scenario, Q_{abs} decreased with cell diameter for 460, 480, and 510 nm (where absorption by secondary carotenoids is very strong), whereas the opposite was true for 620 and 680 nm, where the cellular absorption was much lower.

Regardless of wavelength, Q_{ext} fluctuates with decreasing magnitude as cell size increases, stabilizing at ~30 μm, suggesting wide variation in the range of cell sizes likely to be encountered in the field. Q_{bb} generally decreases with increasing cell diameter; however, this is again modified by low absorption at

Table 2. Pigment Contents Used to Investigate the Impacts of Pigment Mixtures[a]

	Pigment Set 1	Pigment Set 2	Pigment Set 3	Low End-Member Scenario	Medium Pigment Scenario	High End-Member Scenario
Chlorophyll *a* (percent total cell dry mass)	0.5	0.5	0.5	0.1	1	3
Chlorophyll *b* (percent total cell dry mass)	0	0.4	0.4	0.1	0.5	1
Primary carotenoids (percent total cell dry mass)	0.1	0.1	0.26	0.1	1	10
Secondary carotenoids (percent total cell dry mass)	0.5	1.0	1.4	0.1	1	10
Change in α (clean–algal)	0.64–0.63 = 0.01	0.64–0.61 = 0.03	0.64–0.59 = 0.05	0.64–0.59 = 0.05	0.64–0.57 = 0.07	0.64–0.39 = 0.25

[a]We assume that increased chlorophylls are due to chlorophyll *b* rather than chlorophyll *a* (*Remias et al.* [2010] did not determine this empirically). Pigment concentration is expressed as percent total cellular dry mass.

620 nm raising Q_{bb}. These phenomena are exaggerated in the high-pigment scenario and diminished in the low-pigment scenario. This raises an interesting avenue for further research, since Q_{bb} is modified by pigmentation and could possibly be inferred from ratios of backscattered radiation gathered by remote sensing in high-biomass scenarios. We suspect that Lorenz-Mie theory will underestimate backscattering by algal cells because it discounts heterogeneity in cell shape and structure; however, empirical measurements of backscattering by algal cells are scarce, and to our knowledge no data exist for snow algae. These experiments indicate that there is wide variation in cell optics at the scale of individual cells. The following sections report investigations into the effect of pigmentation, cell size, and biomass at the population level on the albedo of snowpacks.

3.1.2. Pigmentation

For pigment mass fractions we were guided by the sparse literature on pigment concentrations in *C. nivalis* and also the analogue species *Chlamydomonas reinhardtii*. For *C. reinhardtii* mass fractions between 0.17 and 2.25% for chlorophyll *a*, 0.13 and 0.70% for chlorophyll *b*, and 0.19 and 0.73% for secondary carotenoids have been reported [*Pottier et al.*, 2005; *Leya et al.*, 2009; *Kandilian et al.*, 2013; *Lee et al.*, 2013; *Yarnold et al.*, 2016]. For *C. nivalis*, chlorophyll:carotenoid ratios as high as 1:20 have been identified in red algae, but this varies dramatically depending upon environmental stresses, in particular light intensity and nutrient deficiency [*Remias et al.*, 2005, 2010; *Lutz et al.*, 2014; *Minhas et al.*, 2016]. We therefore use pigment concentrations between 0 and 3% for chlorophyll *a*, 0 and 1% for chlorophyll *b*, and carotenoid concentrations between 0 and 10% because, on the basis of our literature search, we consider these to encompass a realistic wide range of pigment concentrations that could be encountered in field samples. We used these four key pigments because they are the only ones for which empirical data are available; however, the model is currently capable of incorporating 11 different pigments and could incorporate more when absorption data become available. For albedo calculations we simulated a melting snowpack (SSA = 1 $m^2\,kg^{-1}$ and density = 500 $kg\,m^{-3}$) and used COART irradiance for the Programme for Monitoring of the Greenland Ice Sheet (PROMICE) weather station MIT (Mittivakkat Gletshcer) on a cloudless mid-July day. In all simulations the biomass was high (1 mg^{alg}/g^{snow}) and concentrated into a 1 mm surface layer. This was chosen on the basis of field observations of algal cells inhabiting a thin surface layer of melting snow, providing a physical rationale for the modeled cell depth distribution. However, the finest sampling resolution of empirical studies to date has been 2 cm [*Aoki et al.*, 2011]. The choice of depth distribution is important for the modeling—over an order of magnitude reduction in impurity mass fraction is required to generate the same snowpack albedo when the alga is distributed through 2 cm snow. To demonstrate this, we have repeated our biomass experiments with algae in a 2 cm thick layer and provided these in supporting information S1 for comparison, highlighting the need for careful characterization of the spatial distribution of algal cells in three dimensions for future bioalbedo studies.

As expected, higher concentrations of each pigment result in a greater absorption coefficient with distinct spectral peaks and a reduction in broadband albedo (Figure 3). Furthermore, since real cells contain combinations of pigments that can vary according to environmental conditions, we modeled six pigment mixtures, ranging from a low end-member (all pigments set at 0.01%) to a high end-member (all pigments set at the maximum in the ranges described above). For realistic pigmentation between these end-members, we were guided by laboratory data for *C. nivalis* incubated under different light conditions [*Remias et al.*, 2010]. We use

pigment concentrations measured before (Pigment Set 1) and after a 3 day incubation under high light (Pigment Set 2) and after a 3 day incubation under high light and elevated UV-B (Pigment Set 3), thereby providing pigment sets tractable to real illumination conditions. We also use our medium-pigment scenario created for the Lorenz-Mie experiments. The pigment mass fractions used in each set are provided in Table 2. The high-pigment end-member had the greatest impact upon broadband albedo. Secondary (photoprotective) carotenoids are probably especially important for snow albedo because in real cells they are likely to accumulate at higher concentrations than other pigments; their concentration is sensitive to local environmental conditions, and they have high-absorption coefficients. However, this will be dependent upon bloom maturity and local effects [*Remias et al*., 2010]—indeed, site MIT17 in *Lutz et al.* [2014] showed significantly higher concentration of primary carotenoids than secondary.

3.1.3. Cell Size (χ)

We investigated the impact of cell diameter on spectral and broadband albedo by fixing pigment concentrations, snow physics, and biomass. We again used 1 mg^{alg}/g^{snow} in a 1 mm layer in a melting snowpack (SSA = 1 and density = 500). Our pigment mass fractions selected were between our low- and high-pigmentation end-member scenarios (chlorophyll a = 1.5%, chlorophyll b = 0.5%, primary carotenoids = 1%, and secondary carotenoids = 1%). The impact of cell size upon albedo was thereby calculated for cell diameters between 1 and 40 μm. Microscopy undertaken by previous studies suggest a range of cell diameters ranging from 10 to 35 μm for real red snow algae [*Takeuchi et al*., 2006]. The relationship between cell size and albedo is wavelength dependent, but for these calculations the absorption cross section was calculated at λ = 789 nm because this was the weighted average wavelength of the incoming solar irradiance. Figure 3i shows the spectral albedo along with the change in broadband albedo with increasing cell diameter. Increasing cell size enhances the albedo-reducing effect of the algal blooms. For this specific biomass, snowpack, and pigment combination, increasing the cell size from 1 to 40 μm caused a broadband albedo reduction of 0.14 for a heavy bloom of 1 mg^{alg}/g^{snow}. This range includes extreme lower and upper end-members. Apart from very large (35 μm) cells observed by *Takeuchi et al.* [2006], most studies report *C. nivalis* diameters to be between 10 and 20 μm. As cell diameter increases so does the path length through absorptive material without opportunity for scattering, so there is a physical explanation for larger cell diameters reducing snowpack albedo. We caution that in this model increasing the cell size simply grows the absorptive unit in the snowpack and does not account for scattering effects, which may turn out to be significant, especially in high-biomass, large-cell scenarios. Future research should aim for a rigorous characterization of both absorption and scattering within the snowpack resulting from the growth of snow algal cells.

3.1.4. Biomass

All albedo simulations take into account the optical parameters described in previous sections, which define the proportion of solar energy absorbed and reflected by an algal cell. Of major importance for determining snow albedo is then the number of these cells and their distribution within the snowpack. To isolate the impact of cell concentration from changes in cell size and pigmentation, we held those optical parameters constant and simulated populations of red snow algae with biomass ranging over 6 orders of magnitude between 1 ng^{algae}/g^{snow} and 1 mg^{algae}/g^{snow} (Figure 4). Again, the algae were concentrated in a 1 mm surface layer in a melting snowpack (SSA = 1 $m^2\,kg^{-1}$ and density = 500 $kg\,m^{-3}$). Pigment concentrations and cell size were the same as for the cell size experiments (cell diameter = 20 μm, chlorophyll a = 1.5%, chlorophyll b = 0.5%, primary carotenoids = 1%, and secondary carotenoids = 1%). Biomass concentrations of 1–10 ng^{algae}/g^{snow} had a negligible impact upon snow albedo, whereas a biomass concentration of 1 mg^{algae}/g^{snow} had a greater impact, reducing the broadband albedo to 0.58 (a change of 0.07). The biomass in the upper layer and the broadband albedo were inversely related, and higher biomass caused distinct spectral peaks related to individual algal pigments to be more pronounced. Increasing pigmentation and cell size enhances the effect of additional biomass, such that for the same biomass range with low pigmentation and small cells (diameter = 5 μm; all pigments set at 0.1%), the broadband albedos were reduced by a maximum of just 0.006, and with larger cells and high pigmentation (diameter = 35 μm and secondary carotenoids elevated to 10%), the range of broadband albedos was 0.65 to 0.39 (maximum change 0.26). Therefore, while biomass exerts a primary control upon the impact of algae on snow albedo, the optical properties of the cells themselves are also crucial.

For comparison, we also modeled the albedo impact of adding BC in the same concentration range. Per unit mass, the albedo-reducing effect of BC was greater than any of our algal cells. For our melting

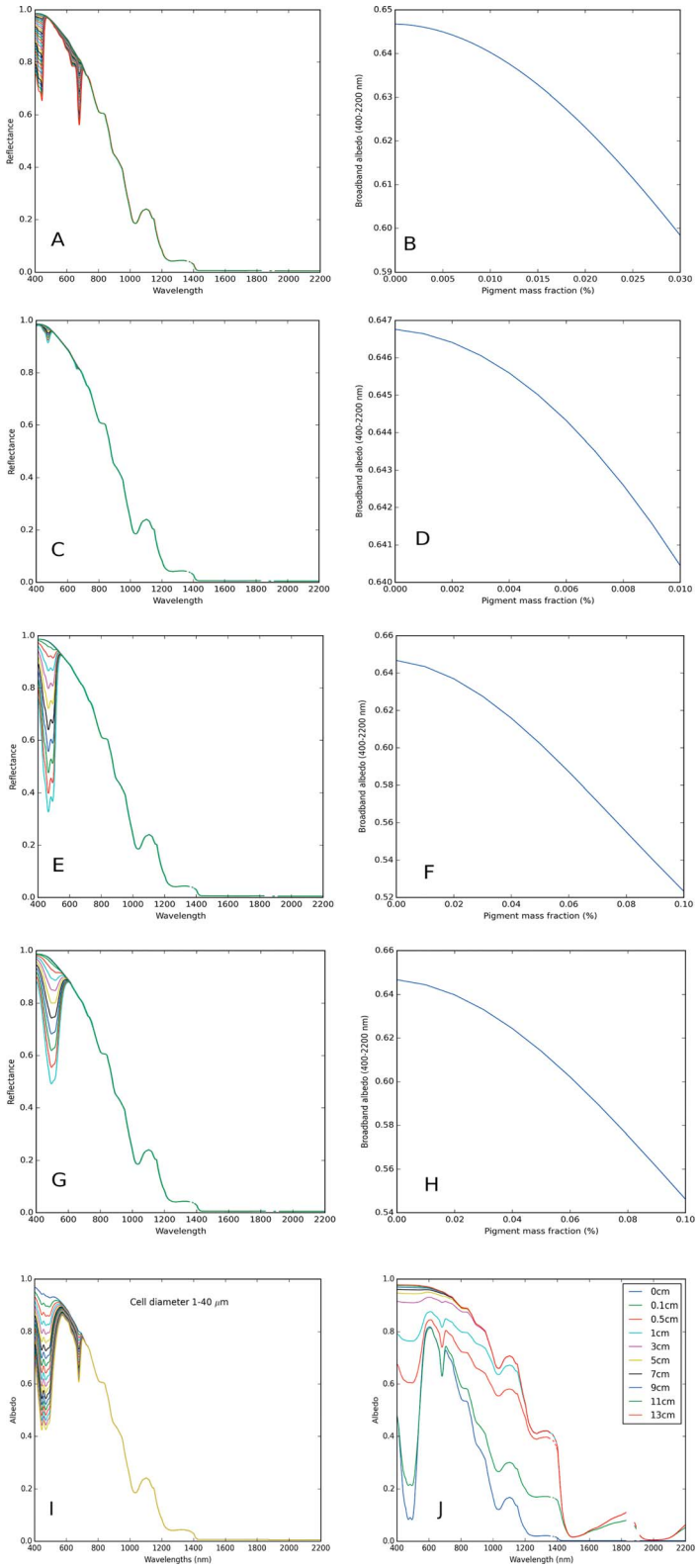

Figure 3. Spectral and broadband albedos for red algae (cell diameter = 20 μm, biomass = 1 $mg_{algae}\ g_{snow}^{-1}$) in 1 mm surface layer of a melting snowpack (SSA = 1 $m^2\ kg^{-1}$, density = 500 $kg\ m^{-3}$) with varying mass fractions of (a and b) chlorophyll *a* (0–3%), (c and d) chlorophyll *b* (0–1%), (e and f) secondary carotenoids (0–10%), and (g and h) primary carotenoids (0–10%). (i) The spectral albedo of the melting snowpack for cell diameters between 1 and 40 μm. (j) The spectral albedo of the melting algal snowpack with varying thickness of overlying fresh snow.

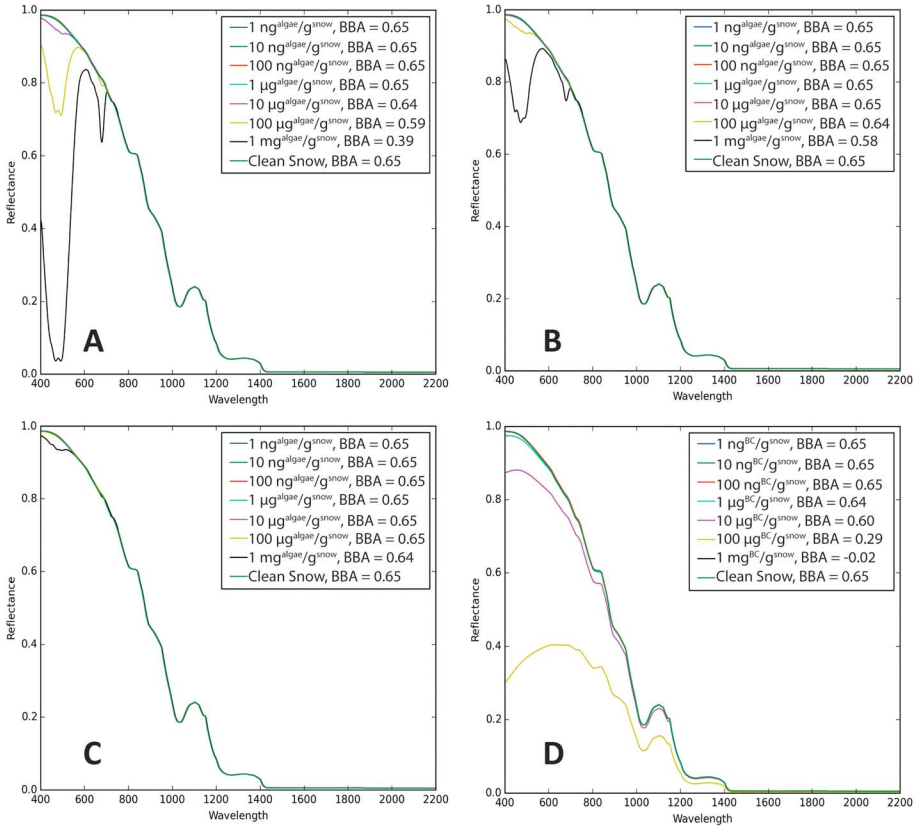

Figure 4. Spectral albedo for biomass ranging from 1 ng^{algae}/g^{snow} to 1 mg^{algae}/g^{snow} for our (a) experimental pigment set, (b) elevated secondary carotenoids, and (c) low pigmentation. (d) Snowpack albedos with varying concentrations of BC are shown. Legend shows the biomass concentration in g^{algae}/g^{snow} and the broadband albedo.

snowpack, the model predicted a broadband albedo of zero for 1 mg^{BC}/g^{snow}, indicating that this concentration of BC is too high for a realistic albedo simulation. For comparison, the same mass of heavily pigmented algae reduced the melting snowpack albedo to 0.39. The impacts of both types of impurity depend upon the snowpack characteristics. For a given impurity load a fresh snowpack has a higher albedo than a melting snowpack due to the increased opportunity for scattering events in the upper layers. For example, we ran the model with a surface layer of fresh snow (SSA = 30 m^2 kg^{-1} and density = 300 kg m^{-3}) and found that the snowpack albedo was 0.82 with no BC, 0.42 with 0.1 mg^{BC}/g^{snow}, and 0.04 with 1 mg^{BC}/g^{snow}.

3.1.5. Hypothetical Heavy Bloom

Based upon our simulations above, we suggest that the most effective scenario for biological albedo reduction is—unsurprisingly—large, heavily pigmented cells at high concentrations in a melting snowpack. We simulated such a scenario using a 1 mg^{algae}/g^{snow} biomass concentration of red snow algae in a 1 mm surface layer with cell size of 35 µm and pigment mass fractions of 3% chlorophyll *a*, 1.5% chlorophyll *b*, 10% primary carotenoids, and 10% secondary carotenoids, which we consider to be high based upon data in *Remias et al.* [2005, 2010] and *Lutz et al.* [2014]. We convolved the spectral BHR of the simulated snowpack with incoming spectral irradiance to produce albedo, which we present spectrally and as a broadband value integrated between 400 and 2200 nm. We used COART to model incoming solar radiation for PROMICE site MIT on Mittivakkat Gletscher (Greenland) because meteorological data are also available for the same day, which we used to drive the energy balance model and estimate melt rate. The impact of this bloom on the snow albedo was a reduction of 0.35, from 0.64 for the clean snowpack to 0.29 for the algal snow, enhancing the local melt rate by 16 mm w.e. d^{-1}. In comparison, a BC concentration of 0.16 mg^{BC}/g^{snow} would be required to have equal effect on broadband albedo. We include this as a suggested upper limit for melt acceleration by biological darkening of snow but reiterate

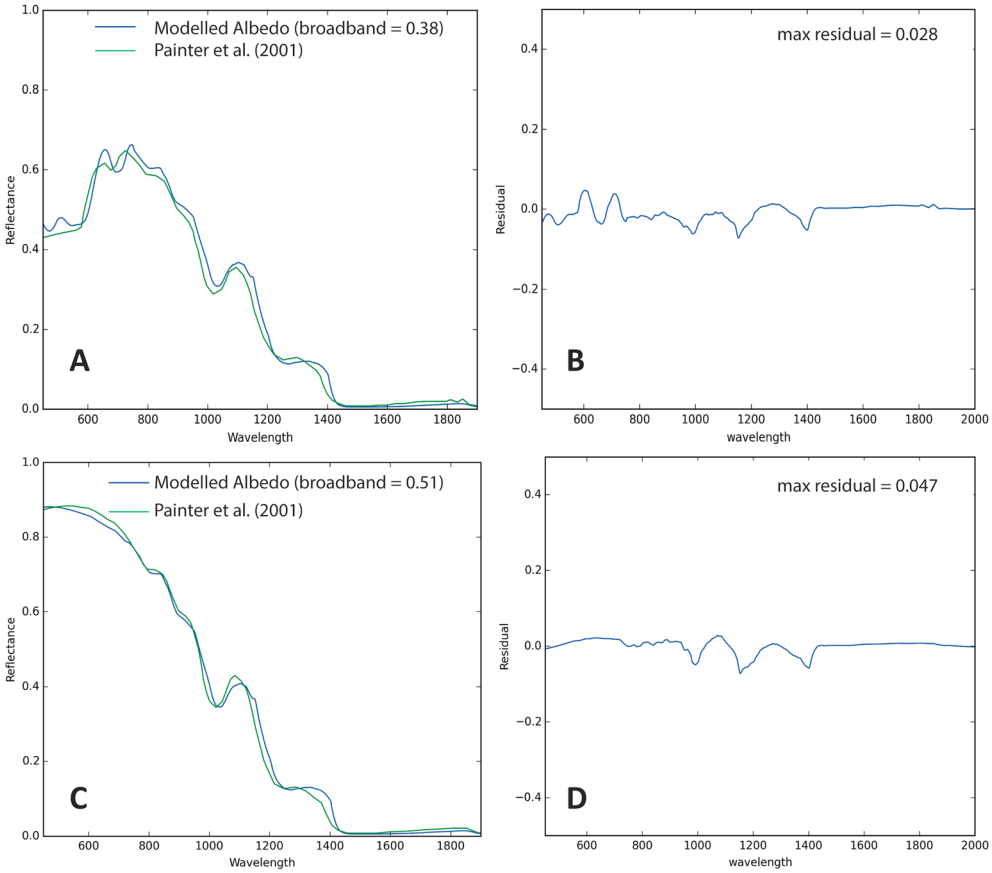

Figure 5. (a) Albedo of algal snow in California from measurements [*Painter et al.*, 2001] and our model simulation for alga-free snow. (b) Residuals for modeled and measured albedo values for clean snow. (c and d) The same data for algal snow.

that the albedo-reducing efficacy of any impurity will vary according to impurity optical properties, snow physics, and irradiance conditions.

3.1.6. Real Bloom: *Painter et al.* [2001]

We used spectral reflectance of algal-free and algal snow in California presented by *Painter et al.* [2001] as target data for forward modeling (Figure 5). We first modeled an abiotic snowpack, tweaking the SSA, density, and BC concentration until the spectral reflectance matched that of the empirical data. The values used were always within a predefined range defined by an extensive literature search (Table 3). A crucial parameter missing from the field data is the distribution of cells within the sampled snowpack. On the basis of published [e.g., *Lutz et al.*, 2014] and our own unpublished field observations, we expect the majority of cells to occupy a very thin (1 mm) layer on the snow surface, although cells can also exist at depth within the snowpack as discussed later in this paper. *Painter et al.* [2001] indicate errors up to 20% for their cell counts. These factors combined make the relation between empirical measurement of cell abundance and cell concentration in the model tenuous, so we treat cell concentration as a variable that was changed iteratively to provide good agreement between modeled and measured data. The same is true of pigment

Table 3. Parameters Used in the *Painter et al.* [2001] Simulation

	SSA ($m^2\ kg^{-1}$)	Density ($kg\ m^{-3}$)	BC g^{BC}/g^{snow}	Biomass g^{alg}/g^{snow}	Pigments (Chl *a*, Primary Carotenoids, Secondary Carotenoids, Phycoerythrin) Expressed as Percent Total Dry Mass	Indirect Effect (BC Equivalent g_{BC}/g_{snow})	Cell Size (μm)	Maximum Residual
Clean snow	3, 3, 4, 5, 5	600	10×10^{-6}	0	0	0	na	0.028
Algal snow	3, 3, 4, 5, 5	600, 600	34×10^{-6}	0.0022	1.5, 0.05, 0.058, 2.8	22×10^{-6}	15	0.011

Table 4. Data From *Lutz et al.* [2014] for Two Red Algal Blooms[a]

Site	Total Chlorophyll	Primary Carotenoids	Secondary Carotenoids	Algal Concentration in Top 1 mm g^{algae}/g^{snow}	BC (Clean Snow) g^{BC}/g^{snow}	BC (Algal Snow) g^{BC}/g^{snow}	α_{vis} (Measured)	α_{vis} (Model)	α (Model)	Melt Rate (mm w.e. d^{-1})
Clean snow	0	0	0	0	1×10^{-9}	1×10^{-9}	0.75	0.75	0.44	39
MIT17	1.3	3.44	0.45	9×10^{-4}	1×10^{-9}	1×10^{-9}	0.57	0.57	0.35	47
MIT19	1.21	0.76	0.68	1.4×10^{-3}	1×10^{-9}	1×10^{-9}	0.39	0.39	0.26	54

[a]Pigment concentrations are expressed relative to chlorophyll *a*.

concentrations, which *Painter et al.* [2001] did not measure. For future modeling studies, it would be very useful to report the dry mass of algal cells per unit mass of snow and especially to characterize the spatial distribution of cells with depth in the top few centimeters of the snowpack. We also noticed that the reflectance was depressed at near-infrared (NIR) as well as visible wavelengths in the field data, which was not replicated by applying biomass alone to the modeled snowpack. This can be explained by (i) the enhanced melt due to algal cells causing interstitial pores to fill with meltwater, thereby increasing their effective grain size; (ii) enhanced surface lowering due to algal cells concentrating inorganic impurities on the ice surface; and (iii) algal cells enhancing the retention of inorganic impurities on the ice surface. These "indirect feedback" impact reflectance at all visible and near-infrared wavelengths and can therefore be combined into one parameter, represented as a quantity of BC, which also absorbs approximately independently of wavelength. Assuming that BC concentrations are equal between nearby sites, the difference in BC concentration required to accurately model alga-free and algal snow at NIR wavelengths can be interpreted as the indirect bioalbedo effect. Understanding of indirect effects of algal cells upon surface reflectance is currently too weak to model physically, so this proxy offers a useful first approximation. Residuals between modeled and measured spectra were obtained by differencing the two curves. A curve was thereby produced that approximated *Painter et al.*'s [2001] data with an error <0.07 in the wavelength range 450 to 2200 nm. Broadband albedo of the snow dropped from 0.51 to 0.38 due to algal biomass, of which 0.07 (53%) was due to direct biological effects and 0.06 (47%) was due to indirect effects.

3.1.7. Real Bloom 2: *Lutz et al.* [2014]

We forward modeled red algal blooms measured on the Greenland Gletscher Mittivakat by *Lutz et al.* [2014], who found the red coloration to be due to resting cysts of chlorophyll and carotenoid-rich *C. nivalis*. We note that *Lutz et al.* [2014] reported broadband albedo measurements that were generated by turning a photosynthetically active radiation (PAR) sensor upward and downward over a sample site, therefore only measuring incoming and reflected radiation between 400 and 700 nm. We integrated the albedo over the visible wavelengths only (α_{vis}) to test the model against *Lutz et al.*'s [2014] data, then expanded the limits of integration (400–2200 nm) to generate more realistic broadband albedo values to drive the melt model (α). We compared α_{vis} to α to demonstrate the magnitude of error arising from presenting PAR reflectance values as broadband albedo.

Melting of *Lutz et al.*'s [2014] observed snowpack was simulated as realistically as possible, using values for wet snow (SSA = 0.1 $m^2\,kg^{-1}$ and density = 600 $kg\,m^{-3}$). This provided a clean snow α_{vis} of 0.75, equal to that measured by *Lutz et al.* [2014]. In the simulations, the algae were concentrated into the upper 1 mm of the snowpack. We assumed that no algae were present in snow beneath the top "algal" layer and that 1 ng^{BC}/g^{snow} was present throughout the snowpack. As for the *Painter et al.* [2001] data, we were limited by a lack of information regarding sampling protocol that compelled us to vary the algal cell concentration in an upper 1 mm layer iteratively, this time using the reported α_{vis} rather than spectral reflectance curves as target data. The pigment concentrations were as reported in *Lutz et al.* [2014] for each site (Table 4). We were able to accurately reproduce the measured α_{vis} to within 0.01 (Table 4). The difference between α and α_{vis} was 0.31 for the alga-free snow, 0.22 for MIT17 and 0.13 for MIT19.

These albedo data were used along with meteorological data for the Gletscher Mittivakkat (SE Greenland) for a 14 day period in midsummer (8–21 July 2012) to coincide with the ground measurements of *Lutz et al.* [2014], which were used to model the real bloom. The data were measured at the station MIT automatic weather station (PROMICE; www.promice.org) on Mittivakkat Gletscher. Solar irradiance was high during this period, and so radiative fluxes dominated the

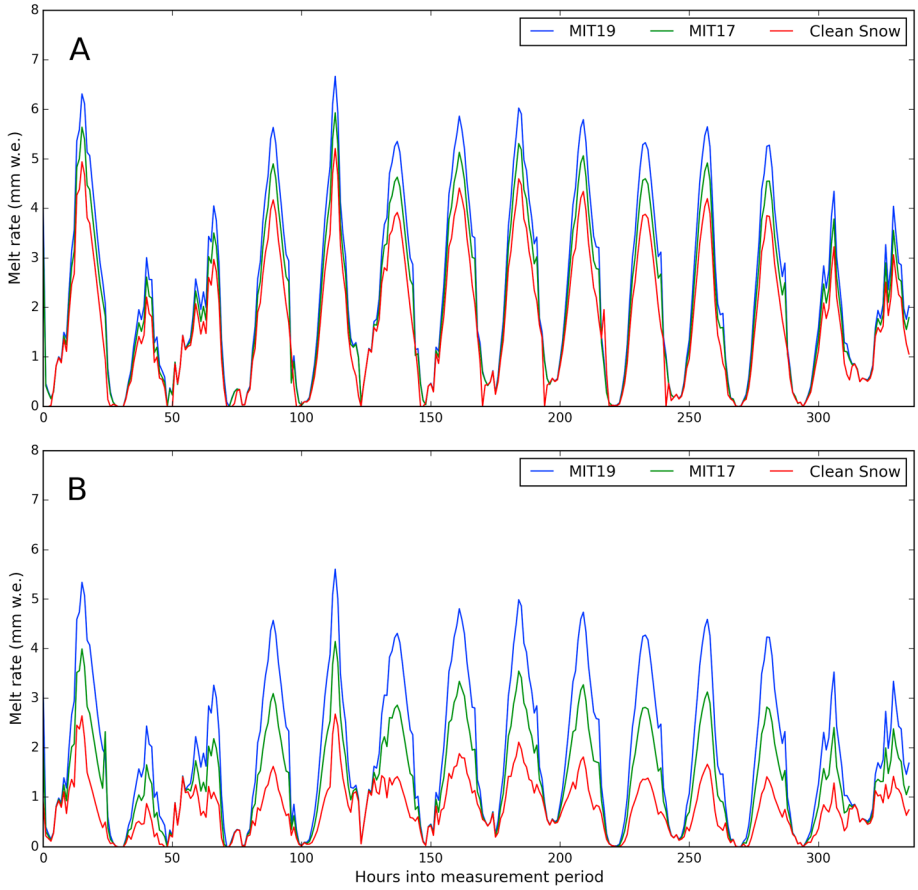

Figure 6. Predicted melt rate for sites on Mittivakat Gletscher. (a) Albedo used to drive the model is a broadband albedo (400–2200 nm). (b) Albedo values are integrated over the visible wavelengths only. The meteorological data are provided in our open repository. In particular, we note that the lower melt days early and late in the observation period coincided with periods of low incoming shortwave radiation.

surface energy balance, thereby providing favorable conditions for albedo-induced surface ablation. Vapor pressure data were calculated using the method of *Tetons* [1930]. We held these meteorological data constant and varied α to determine the rate of surface melt attributable to algal blooms with different optical properties.

The clean snow measured by *Lutz et al.* [2014] was melting at a rate of 39 mm w.e. d^{-1} over the measurement period, compared to 47 mm w.e. d^{-1} at site MIT17 and 54 mm w.e. d^{-1} at MIT19 (Figure 6). Our model therefore indicates a melt enhancement due to the presence of algal blooms of 8 and 15 mm w.e. d^{-1} (or 1.2- and 1.4-fold increase) for the two sites. Using albedo integrated only over the visible wavelengths, the model predicted melt enhancement of 18 mm w.e. d^{-1} and 31 mm w.e. d^{-1}. Omitting the NIR wavelengths overestimated the snow albedo and therefore underestimated melt rate for clean and algal snow (Figure 6). However, since only the wavelengths most affected by algae were measured it also overestimated the biological albedo-reducing effect. Overestimating albedo by integrating only over the visible wavelengths was also demonstrated empirically on sea ice by *Zatko and Warren* [2015]. The closest physical analogue in their study was the deep slush, which showed α_{vis} of 0.78 compared to α of 0.51, which is very similar to our estimates for the "clean" Mittivakkat snow.

3.1.8. Subsurface Blooms

We also used our model to simulate the impact of cells existing at depth within the snowpack (Figure 2j). The impact of subsurface blooms on snow albedo has not yet to our knowledge, been modeled, but their existence has been reported in Californian snow [*Thomas*, 1972]. We therefore adapted our model to simulate algal blooms at various depths within a snowpack with the same range of optical parameters and

biomass concentration as for the biomass experiments described above. We found that the thickness of overlying snow required to eliminate the albedo-reducing effect of an algal bloom varies with the optical properties of the algae and the total biomass, as well as with the physical characteristics of the overlying snow. Blooms may well become buried by fresh snowfall (SSA = 30 $m^2 kg^{-1}$ and density = 250 $kg m^{-3}$), which is very effective at obscuring the underlying algal bloom (a layer 13 cm thick raised the albedo of a melting snowpack with our high end-member "heavy bloom" by 0.44, making it indistinguishable from an alga-free snowpack; Figure 2j). For comparison, we ran the same experiment with our small, low-pigment cells, without changing the biomass concentration. In this case, 8 cm of fresh snowfall was required to completely eliminate the albedo-reducing effect of the bloom. As expected, the biomass concentration strongly influences the thickness of fresh snow through which blooms have an albedo effect. For our heavily pigmented cells, the thickness of overlying snow required to eliminate the albedo-reducing effect of the bloom increased from 1 cm to 13 cm as the biomass concentration increased from 10 $\mu g^{alg}/g^{snow}$ to 1 mg^{alg}/g^{snow}. For our low-pigment cells the range of snow thickness required was 1 mm to 4 cm for the same biomass range. This indicates that depending upon the optical properties of the cells and their biomass concentration, they may alter the albedo of a snowpack even when buried by fresh snow. In our upper end-member, the algal bloom influenced surface albedo under 13 cm of fresh snow. Since blooms are features of melting snowpacks, any overlying fresh snowfall is likely to decay. In this case, the changing physical properties of the snow change the albedo impact of the buried bloom. The large, heavily pigmented cells under 13 cm of decaying snow (SSA = 5 $m^2 kg^{-1}$ and density = 450 $kg m^{-3}$) still reduced the snowpack albedo by 0.02, whereas they had no effect under the same thickness of fresh snow. Similarly, *Aoki et al.* [2011] undertook similar simulations for subsurface BC, also finding the effect to be larger in melting snow compared to fresh snow.

3.1.9. Signature Spectra

Spectral reflectance data are not currently available for blooms of known biomass and snow physics; however, our model can predict it. Different pigments have peak absorption at specific wavelengths, so their presence (and possibly concentration) can be inferred from the shape of reflectance spectra. This could be used to extract ecological information from remotely sensed spectra, since pigmentation can change in response to environmental conditions [*Remias et al*., 2005, 2010]. In particular, *C. nivalis* in its developmental stage contains fewer carotenoids and has a greener coloration; mature cells accumulate secondary carotenoids and become orange-red [*Holzinger et al*., 2016]. We therefore predicted the spectral reflectance of a range of algal blooms and identified "signature" reflectance patterns. Our simulations show that both increasing the number of pigment-containing cells in the snowpack and increasing the pigment concentration in each cell enhance radiation absorption within characteristic wavelengths and result in identifiable deviations from the smoothly convex spectral reflectance curve associated with pure snow. In Figure 2a, predicted spectral reflectance curves of a melting snowpack inoculated with cells containing various concentrations of chlorophyll *a* are shown. The "uniquely biological" spectral signature (absorption peaks at 440 and 680 nm) was identified by *Painter et al.* [2001] as being the result of chlorophyll *a* absorption, which is corroborated by our simulations. The spectral reflectance curves are shown in Figure 1, and the characteristic absorption features associated with each pigment are provided in Table 3. Figure 4 shows the spectral reflectance curves for snow inoculated with cells with mixtures of several pigments with varying biomass concentrations between 1 ng^{algae}/g^{snow} and 1 mg^{algae}/g^{snow}. Several absorption peaks (manifest as reflectance minima) can be identified, in particular the broad absorption feature between 400 and 520 nm resulting from absorption by secondary carotenoids, the twin maxima at 440 and 680 due to chlorophyll *a*, and although the 475 peak contributed by chlorophyll *b* is obscured by the secondary carotenoids, its presence is indicated by its secondary peak at 650 nm.

BC does not preferentially absorb with such distinct spectral peaks. Thin overlying snow and grain evolution can mimic the spectral effects of BC contamination, making separation of BC and snow physics very difficult from spectral data [*Warren*, 2013]. This is supported by our simulations. The broad wavelengths over which BC is effective and the lack of distinctive spectral absorption peaks make it unlikely to obscure the spectral signature of algal cells, although due to its high potency as an albedo reducer, it will significantly reduce α overall when present in sufficient concentrations. These properties also allow us to represent the combined indirect effects of biomass on spectral reflectance as a BC equivalent, until the specific physical mechanisms are better understood.

The burial of an algal bloom beneath a growing layer of fresh snowfall resulted in the gradual attenuation of the characteristic absorption peaks. However, the characteristic spectral reflectance patterns resulting from chlorophyll *a*, chlorophyll *b*, and secondary carotenoids were still discernible for snow cover up to ~8 cm thick for a heavy (1 mg^{algae}/g^{snow}) bloom.

4. Discussion

We have presented a physically based model for the albedo and melt impact of algal growth and blooms within snow cover. The limitations of our model will be examined first in the following discussion. Then, we discuss the biooptical outputs of the model and examine the role of algal blooms in driving melt.

4.1. Model Validity

This melt model is the first to incorporate biological forcing and is predictive, given cell size and pigment concentration, along with snow physical properties and meteorological data. The model could readily be expanded to incorporate additional algal species or pigment types. We do not currently have sufficient empirical data to fully validate the model; however, we note that each section of the model represents an adapted form of a model previously formulated and validated in the literature [*Pottier et al*., 2005; *Libois et al*., 2013; *Brock and Arnold*, 2000]. There are no known empirical data sets that include all the necessary observations required to truly validate our model. We intend to collect our own field data for this specific purpose. This paucity of data along with the current interest in bioalbedo highlights a community requirement for standardized biological and glaciological measurements. Nevertheless, there exist several partial data sets we were able to use (filling information gaps with predicted or literature values) that allow us to make comparisons between field and modeled data. Two data sets were employed for this purpose: *Painter et al*.'s [2001] spectral reflectance data from algal snow in California and *Lutz et al*.'s [2014] broadband measurements from Mittivakkat Gletscher. Both studies quantify cell concentrations in snow but crucially omit information regarding the distribution of these cells in the snowpack. Qualitative descriptions in these papers, along with our own field observations, suggest that the majority of the cells are likely to be concentrated within a 1 mm surface layer, but the field samples likely included snow between the surface and several centimeter depth. This is important for the model as a given number of cells has a greater impact on albedo when concentrated on the snow surface than when distributed through a depth profile in the snow. Furthermore, these studies only provide qualitative descriptions of the snow physics at their field sites. Since our model is built upon well-known snow radiative transfer equations that have been well tested, we are confident in its ability to simulate snow physics. There is also no quantitative assessment of inorganic impurities such as BC in the snowpack. These unknown parameters had to be estimated within sensible ranges, guided by existing literature. For example, SSA and density of melting snow have been characterized by *Domine et al.* [2006], *Gallet et al.* [2009], *Yamaguchi et al.* [2014], and *Matzl and Schneebeli* [2006] among others. We therefore present these analyses to demonstrate the utility of our model for both forward and inverse modeling of algal snow albedo and to illustrate the need for a standardized suite of bioalbedo measurements in field studies. Full model validation must wait until we have undertaken field work for this specific purpose.

Several assumptions in the model formulation require justification. First, for the application of the well-known Lorenz-Mie solution (which solves Maxwell's equations for photon interactions with small spheres), we assume that the cells comprising the algal blooms are spherical and homogeneous, which is likely justifiable for *C. nivalis*. For other species of algae, for example, filamentous cyanobacteria, this assumption may not be valid, and an alternative method, for example, the *T*-matrix method [*Waterman*, 1965], could be employed. The assumption of homogeneity requires that pigments are the only absorbing entities within the cell and that no light is absorbed by the cell wall, membrane, or any organelles. This is a simplification, although light absorption by cellular material other than pigments is considered negligible [*Uličný*, 1992]. The analysis of single-cell optical parameters has been attempted here using Lorenz-Mie theory for homogenous spheres; however, it may turn out to be more appropriate to use models that consider concentric spheres of varying refractive index [e.g., *Quirantes and Bernard*, 2004]. In our albedo modeling, we also make the assumption that scattering by algal cells is negligible compared to that of the surrounding snow grains because snow grains are highly scattering and the cell concentrations are relatively low, as has been justified by several previous studies [e.g., *Stamnes and Stamnes*, 2016; *Zatko et al.*, 2013]. However, future versions of the model

should determine this for algal cells specifically by integrating the Lorenz-Mie scheme directly into the RTM. The assumption that cells do not alter the scattering cross section of the snowpack will weaken as cell size and biomass increase, so future model development should focus upon a more rigorous characterization of cell diameter. Our approach is beneficial in terms of computational simplicity but limits our model to dispersions of cells within layers of snow and prohibits us from studying processes associated with very high biomass concentrations including self-shading in thick algal layers and flocculation. *Aoki et al.* [2013] also used this assumption when applying a mineral-dust model to an algal snow radiative transfer scheme. It is interesting to compare their approach to ours, since they retrieved the spectral absorption coefficient for ice algal cells from spectral measurements, whereas we have built it from user-defined variables. Data in *Aoki* [2013] indicate that both methods have predicted spectral absorption coefficients for red snow algae within the same order of magnitude.

Finally, we note that our model only considers absorption by algal cells at wavelengths greater than 400 nm. We consider this to be reasonable, given that absorption by algal cells is concentrated between 400 and 700 nm. However, we also note that recent literature has highlighted the role of UV-screening compounds, such as scytonemin, as significant albedo reducers in soils [*Couradeau et al*., 2016]. Therefore, future versions of this model may include shorter wavelengths as the biological basis behind absorption at UV wavelengths becomes better understood.

4.2. Biooptical Properties of Red Snow Algae

The absorption of light within an algal cell is controlled by the cell size and the concentration of intracellular pigments. Our biooptical model indicates that secondary carotenoid concentration has the greatest effect upon the absorption of light within the cell, which is not surprising given their greater in vivo absorption coefficient (Figure 1). However, for all four pigment types (chlorophylls *a* and *b* and primary and secondary carotenoids), increasing the pigment concentration increased the cell's absorption coefficient, making it a more effective absorber of visible light. This reduced the albedo of the snowpack and caused it to melt faster in our simulations. In addition, increasing cell diameter caused the absorption efficiency to increase and scattering efficiency to decrease (due to addition of absorptive medium and a lower frequency of photon transition between media of different density when cells are larger). While this may be an important process for cells in open water or bioreactors, scattering in a snowpack is overwhelmingly dominated by the optical properties of snow crystals and minimally impacted by the presence of impurities and is therefore discounted by TARTES. Our modeling therefore confirms the results of several previous studies that find pigmentation and cell size to be key determinants of the optical properties of small, spherical algal cells [*Pottier et al*., 2005; *Lee et al*., 2013; *Dauchet et al*., 2015]. Larger cells with higher-pigment contents will be most effective as absorbers of solar energy and will have greatest impact upon snowpack albedo and melt rates. Changes in biooptical properties also changed the modeled Lorenz-Mie efficiency factors, which may facilitate remote detection of some snow-algal ecological information.

4.3. Impact of Algal Blooms on Snow Albedo

The biomass of algal cells present in the snowpack had a greater effect on the snowpack α than changes in pigment concentration. An upper end-member heavy bloom of 1 mg^{algae}/g^{snow} was simulated (where chlorophyll *a*, chlorophyll *b*, and secondary carotenoid concentrations were all high), which reduced the albedo of the snowpack by 0.35. We compared algal blooms to BC deposition, finding that 1 mg^{algae}/g^{snow} had an equivalent impact on α to 16 $\mu g^{BC}/g^{snow}$. Previous measurements of BC in Greenland snow from Summit, Dye-3, and Camp Century suggest a range of 1–15 ng^{BC}/g^{snow} to be realistic [e.g., *Slater et al*., 2002; *Cachier*, 1997; *Chylek et al*., 1995; *Cachier and Pertuisol*, 1994], although more measurements at additional sites across the ice sheet are needed to constrain spatial and temporal variations. It is well known that BC is a powerful albedo reducer on snow and ice [*Goelles et al*., 2015] and historically may have terminated the Little Ice Age [*Painter et al*., 2013]; we therefore suggest that α is much more sensitive to BC than to an equal concentration of algal blooms. However, if measured BC concentrations of 1–15 ng^{BC}/g^{snow} are representative for Greenland snow, algal blooms may contribute more to albedo decline. Algal blooms have been reported covering large areas on snowpacks worldwide [e.g., *Hisakawa et al*., 2015], and hence, alga is likely to be a crucial impurity that must be considered in predictions of snow albedo and melt.

Indirect impacts of algae on spectral reflectance may enhance the albedo-reducing effect further. Albedo is very sensitive to grain size, since smaller discrete grains provide more opportunities for scattering of photons out of the snowpack [e.g., *Wiscombe and Warren*, 1980; *Nolin and Dozier*, 2000; *Kokhanovsky and Zege*, 2004; *Xie et al*., 2006]. Meltwater accumulation in pore spaces is approximately equivalent to increasing snow grain size, since it replaces air-ice interfaces with water-ice interfaces, promoting forward scattering and decreasing the likelihood of a photon scattering out of the snowpack. Similarly, algal blooms might enhance the longevity of BC and dust on the snow surface (e.g., by aggregating inorganic material to form cryoconite [*Takeuchi et al*., 2001; *Langford et al*., 2010]), offering another mechanism of biological melt acceleration. Therefore, while the direct effect of algae is clearly important, their indirect impacts may also be significant. In this paper, due to the current lack of research into physical mechanisms of indirect effects of algal biomass on spectral reflectance, we consider all indirect effects in one combined BC-equivalent parameter. Our modeling, using *Painter et al*.'s [2001] field data, suggests that up to half of the albedo reduction due to algal cells may be due to indirect feedback effects.

4.4. Melt

Biomass concentration on the surface of the snowpack altered the rate of snowmelt for a Greenland glacier. We attributed 8 and 15 mm w.e. d^{-1} at Mittivakkat Gletscher sites MIT17 and MIT19 to the direct albedo influence of algal blooms (Figure 6). Photoacclimation and cell accumulation over the course of a melt season may have an appreciable impact upon total snowmelt from a snowpack and should therefore be accounted for in melt models, given that pigment concentrations are shown to impact on the biooptics of the cells and therefore the spectral and spectrally integrated albedo. We note that much more research is needed to constrain likely pigment concentrations in snow algae under varying light, temperature, and nutrient conditions. Many factors influence surface melt, and a linear extrapolation of our simulated melt enhancement to the glacier scale is not appropriate without high-resolution mapping of snow physical characteristics and impurity content, along with detailed meteorological data. The melt simulations presented here were for clear-sky days in mid-July, meaning that radiative processes likely dominated the surface energy balance and the snow was particularly sensitive to changes in albedo. While these conditions may be typical for some locations (e.g., SW Greenland), the relationship between albedo and melt rate will vary under different meteorological conditions. We present these melt simulations to illustrate the potential for extracting melt rate information from integrated biooptical, radiative transfer, and energy balance modeling frameworks; however, in-depth analysis of the melt time series is beyond the scope of this paper. For interested readers, we provide the melt and meteorological data in our repository (https://bitbucket.org/jmcook/bioalbedo_0.1/overview). Overall, our simulations do suggest a significant impact of algal blooms upon snowmelt, and therefore, bioalbedo should be studied in more detail to support melt forecasting.

4.5. Real Blooms

To our knowledge there are no published data sets that quantitatively describe both the physical and biological characteristics of a snowpack. Therefore, we are currently unable to fully validate our model. We can only propose to provide a full validation in a follow-up paper after undertaking our own field work. Given the current interest in bioalbedo, we also intend to provide a clear manifesto for bioalbedo measurements in a follow-up paper that will promote clarity and compatibility between field studies and facilitate both forward and inverse modeling using the scheme we present here. Despite the current lack of data, we were able to apply our model to two partial data sets—one spectral and one broadband—filling missing data with surrogates derived from wider literature. We present these comparisons for two reasons: first, to show that the model is capable of accurately recreating empirical spectral reflectance data given realistic input data; second, since we started with measured spectra and have inferred values for several input parameters, we suggest that the model can be inverted to determine (for example) biomass and pigment concentrations.

For *Painter et al*.'s [2001] data set, we were able to recreate the snow spectral reflectance with a maximum error of 0.07. The error was greatest in the visible wavelengths due to the reflectance varying more at these wavelengths in the model than in the real data. This is probably due to the assumption that pigments are the only absorbing features in the cells and the limited number of pigments in the model. Further experimentation may justify the use of a smoothing function to remove some of this variability in future versions of the model. In both algal and clean snow, there were peaks in the residuals at three points in the NIR wavelengths,

Table 5. Characteristic Spectral Reflectance Features and Ecological Significance of Each Algal Pigment

Pigment	First Absorption Peak	Second Absorption Peak	Curve Characteristics	Ecological Significance
Chlorophyll *a*	440	680	Absorbs strongly in two clear, narrow wavebands	Universal light-absorbing pigment useful as a general biomarker for photosynthetic life
Chlorophyll *b*	475	650	Absorbs strongly in two clear, narrow wavebands	Often elevated in shade-adapted organisms
Primary carotenoids	480	na	Absorb strongly across a wide wave band	Expand the photosynthetic wave band
Secondary carotenoids	460	na	Absorb strongly across a wide wave band	Thought to be a photoprotective response to high light exposure
Phycocyanin	610	na	Absorbs across a wide wave band (350–700 nm) with minimum absorption at 460 nm, gradually rising to maximum at 610 nm	Characteristic of cyanobacteria, used to expand photosynthetic wave band
Phycoerythrin	450	525, 575	"Table-shaped" absorption spectrum with a sharp increase in absorption at 420 nm, plateau with a characteristic "triple-peak" morphology to a sharp drop at 580 nm	Characteristic of red algae, used to expand the photosynthetic wave band

likely due to biological feedback not accounted for in the model or grain size inhomogeneity. Nevertheless, the error overall is small, indicating that the model can recreate real spectra using realistic input values.

Our melt modeling using *Lutz et al.*'s [2014] data shows that our model can be applied usefully even when only broadband albedo values are available. It was used here to expand the PAR albedo measured by *Lutz et al.* [2014] into a more useful broadband value, which could then drive melt modeling. Furthermore, inverting the model can facilitate the "backfilling" of biological or physical measurements missing from empirical data sets. We emphasize that there is currently no empirical data set that includes all the required parameters for completely accurate forward or inverse modeling of snow albedo; however, we suggest that a physical modeling approach enhances the usefulness of partial data sets. With more complete data sets, more reliable modeling can be undertaken.

4.6. Subsurface Blooms

The existence of a photic zone in snow and ice, where PAR penetration sustains photoautotrophy, has been identified by several studies for both ice and snow [*Thomas*, 1972; *Irvine-Fynn et al.*, 2012; *Hodson et al.*, 2013] and the existence of subsurface algal blooms in snow has been confirmed empirically [*Thomas*, 1972]; however, their impact on α has not previously been modeled. We find that subsurface blooms of 1 mg^{algae}/g^{snow} (with high chlorophyll *a*, chlorophyll *b*, and secondary carotenoid concentrations) can impact α of a fresh, clean snowpack at depths up to 0.13 m (Figure 3j). This suggests that the subsurface blooms measured by *Thomas* [1972], which occurred at 10 cm depth in a snowpack in California (USA), could have influenced the surface albedo. Interestingly, *Thomas* [1972] separately observed red discoloration of snow to a depth of 30 cm, implying the existence of biological light-absorbing impurities that could be important factors in radiative transfer in snow. It is not clear whether these exited at depth due to active migration, percolation with meltwater, or burial by snowfall. Many more measurements of subsurface algal cells are required to determine their prevalence in snow worldwide and their effect on snow evolution. There have been suggestions that algal cells employ motility strategies to migrate upward or downward through snowpacks to reach favorable irradiance conditions [*Dove et al.*, 2012] and surface blooms could be buried by summer snowfall. Our model shows that proximity to the snow surface enhances the impact of algal blooms upon surface reflectance, suggesting that shallow subsurface blooms may influence radiative transfer in snowpacks and could be identifiable from remotely sensed spectral data.

5. Signature Spectra

Our simulations indicate the existence of distinct spectra for different impurities within the snowpack, and suggest that impurity type and concentration could be derived from remotely sensed spectral data from orbital or suborbital platforms, even when buried under thin layers of fresh snowfall (Figure 3j) or when mixed with inorganic impurities. The notion of uniquely biological spectral reflectance patterns has been discussed by *Painter et al.* [2001], who identified the absorption feature centred at 680 nm as characteristic of

chlorophyll *a* and therefore photoautotrophic life in snow. We corroborate this using our model and also point to other characteristic absorption features that could be used to extract more detailed ecological information from spectral reflectance data. These are summarized in Table 5.

Our model indicates that these characteristic absorption features may be distinguishable in remotely sensed spectral reflectance data. Pigmentation is dynamic is response to environmental conditions [e.g., *Remias et al*., 2005], and variations in the spectral reflectance over time may provide a means of extracting ecological information regarding stress responses in algal cells. While there are many complicating factors in real snowpacks, our modeling approach indicates that time series of remotely sensed spectral reflectance data offers the opportunity for detecting life in snow and ice, mapping impurities, and forecasting melt. A similar approach could potentially be employed in the search for extraterrestrial photosynthetic life on icy planets and moons.

6. Conclusions and Outlook

We have presented, for the first time, a model of snow albedo and melt that takes into account snow algal blooms. The model provides biooptical, albedo, and melt predictions, given input values for cell size, pigment concentration, biomass loading in the snow, snow physical properties, and meteorological variables. Our model demonstrates that algae can melt snow via a bioalbedo effect and makes the first known quantification of this effect using physical modeling. We also note that this impact is likely amplified by indirect feedback effects that are yet to be characterized but are likely crucial for determining biological melt acceleration. We compared the influence of algal blooms to that of BC on snow albedo, finding that although BC is a more potent albedo reducer than algae per unit volume, algae are likely to accumulate in higher concentrations and therefore have a greater albedo-reducing effect (although the spatial extent of blooms is unknown). In this study, because we are interested in isolating the role of algal blooms, we have not examined the role of dusts which will also often have albedo-reducing effects on snowpacks. The model was also used to predicting spectral reflectance patterns from algal snow, demonstrating the potential for remotely sensed spectral reflectance data for detecting life in the cryosphere and predicting snowmelt.

Acknowledgments

All authors acknowledge UK-funded Natural Environment Research Council Consortium Grant "Black and Bloom" (NE/M021025/1). J.C. acknowledges the Rolex Awards for Enterprise. The authors cite no conflict of interest. Data supporting our conclusions can be found within this manuscript. Codes were written in Python 3.4.3 using packages in the Anaconda 2.3.0 (64 bit) distribution plus TARTES 0.9.3 (http://lgge.osug.fr/~picard/tartes/). Annotated scripts are openly available at https://bitbucket.org/jmcook/bioalbedo_0.1/src. Mie scattering parameters were calculated using MiePlot version 4.6 [*Laven*, 2006]. Details of the Black and Bloom Team can be found at http://blackandbloom.org. In particular, Tristram Irvine-Fynn, Liane Benning, and Steffi Lutz are thanked for comments on manuscript drafts. Two anonymous reviewers were extremely helpful in refining this manuscript.

References

Aoki, T., A. Hachikubo, and M. Hori (2003), Effects of snow physical parameters on shortwave broadband albedos, *J. Geophys. Res.*, *108*(D19), 4616, doi:10.1029/2003JD003506.

Aoki, T., K. Kuchiki, M. Niwano, Y. Kodama, M. Hosaka, and T. Tanaka (2011), Physically based snow albedo model for calculating broadband albedos and the solar heating profile in snowpack for general circulation models, *J. Geophys. Res.*, *116*, D11114, doi:10.1029/2010JD015507.

Aoki, T., K. Kuchiki, M. Niwano, S. Matoba, J. Uetake, K. Masuda, and H. Ishimoto (2013), Numerical simulation of spectral albedos of glacier surfaces covered with glacial microbes in northwestern Greenland, *AIP Conf. Proc.*, *1531*, 176, doi:10.1063/1.4804735.

Benning, L. G., A. M. Anesio, S. Lutz, and M. Tranter (2014), Biological impact on Greenland's albedo, *Nat. Geosci.*, *7*, 691, doi:10.1038/ngeo2260.

Bidigare, R. R., M. E. Ondrusek, J. H. Morrow, and D. A. Kiefer (1990), In vivo absorption properties of algal pigments, in *Ocean Opt ~ cs X, Proc Soc. photo-opt. Instrum. Eng*, vol. 1302, edited by R. W. Spinrad, pp. 90–302 .

Bond, T. C., and R. W. Bergstrom (2006), Light absorption by carbonaceous particles: An investigative review, *Aerosol Sci. Tech.*, *40*(27–67), 2006.

Brandt, R. E., S. G. Warren, and A. D. Clarke (2011), A controlled snowmaking experiment testing the relation between black carbon content and reduction of snow albedo, *J. Geophys. Res.*, *116*, D08109, doi:10.1029/2010JD015330.

Brock, B. W., and N. S. Arnold (2000), A spreadsheet-based (Microsoft Excel) point surface energy balance model for glacier and snow melt studies, *Earth Surf. Processes Landforms*, *25*, 649–658, doi:10.1002/1096-9837(200006)25:6<649::AID-ESP97>3.0.CO;2-U.

Brun, E., E. Martin, V. Simon, C. Gendre, and C. Coleou (1989), An energy and mass model of snow cover suitable for operational avalanche forecasting, *J. Glaciol.*, *35*, 333–342.

Budyko, M. I. (1969), The effect of solar radiation variations on the climate of the Earth, *Tellus*, *21*, 611–619, doi:10.1111/j.2153-3490.1969.tb00466.x.

Cachier, H. (1997), Particulate and dissolved carbon in air and snow at the Summit site, in *Transfer of Aerosols and Gases to Greenland Snow and Ice: Final Technical Report*, pp. 21–27, Cedex, France.

Cachier, H., and M. H. Pertuisol (1994), Particulate carbon in Arctic ice, *Anal. Mag.*, *22*, M34–M37.

Chylek, P., B. Johnson, and P. A. Damiano (1995), Biomass burning record and black carbon in the GISP2 ice core, *Geophys. Res. Lett.*, *22*(2), 89–92, doi:10.1029/94GL02841.

Clarke, A. D., and K. J. Noone (1985), Soot in the Arctic snowpack: A cause for perturbations in radiative transfer, *Atmos. Environ.*, *19*, 2045–2053, doi:10.1016/0004-6981(85)90113-1.

Couradeau, E., U. Karaoz, H. C. Lim, U. Nunes da Rocha, T. Northern, E. Brodie, and F. Garcia-Pichel (2016), Bacteria increase arid-land soil surface temperature through the production of sunscreens, *Nat. Commun.*, *7*(10373), doi:10.1038/ncomms10373.

Dauchet, J., S. Blanco, J.-F. Cornet, and R. Fournier (2015), Calculation of radiative properties of photosynthetic microorganisms, *J. Quant. Spectrosc. Radiat. Transf.*, *161*, 60–84.

Domine, F., R. Salvatori, L. Legagneux, R. Salzano, M. Fily, and R. Casacchia (2006), Correlation between the specific surface area and the short wave infrared (SWIR) reflectance of snow, *Cold Reg. Sci. Technol.*, *46*, 60–68.
Dove, A., J. Heldmann, C. McKay, and O. Toon (2012), Physics of a thick seasonal snowpack with possible implications for snow algae, Arctic, *Arct. Antarct. Alp. Res.*, *44*(1), 36–49.
Edwards, H. G. M., L. F. C. de Oliveira, C. S. J. Cockell, C. Ellis-Evans, and D. D. Wynn-Williams (2004), Raman spectroscopy of senescing snow algae: Pigmentation changes in an Antarctic cold desert extremophile, *Int. J. Astrobiol.*, *3*, 125–129, doi:10.1017/S1473550404002034.
Flanner, M. G., and C. S. Zender (2006), Linking snowpack microphysics and albedo evolution, *J. Geophys. Res.*, *111*, D12208, doi:10.1029/2005JD006834.
Flanner, M. G., C. S. Zender, J. T. Randerson, and P. J. Rasch (2007), Present-day climate forcing and response from black carbon in snow, *J. Geophys. Res.*, *112*, D11202, doi:10.1029/2006JD008003.
Gallet, J.-C., F. Domine, C. S. Zender, and G. Picard (2009), Measurement of the specific surface area of snow using infrared reflectance in an integrating sphere at 1310 and 1550 nm, *The Cryosphere*, *3*, 167–182, doi:10.5194/tc-3-167-2009.
Gallet, J.-C., F. Domine, and M. Dumont (2014), Measuring the specific surface area of wet snow using 1310 nm reflectance, *The Cryosphere*, *8*, 1139–1148, doi:10.5194/tc-8-1139-2014.
Gardner, A., and M. Sharp (2010), A review of snow and ice albedo and the development of a new physically based broadband albedo parameterization, *J. Geophys. Res.*, *115*, F01009, doi:10.1029/2009JF001444.
Goelles, T., C. E. Bøggild, and R. Greve (2015), Ice sheet mass loss caused by dust and black carbon accumulation, *The Cryosphere*, *9*, 1845–1856, doi:10.5194/tc-9-1845-2015.
Grenfell, T. C., and S. G. Warren (1999), Representation of a nonspherical ice particle by a collection of independent spheres for scattering and absorption of radiation, *J. Geophys. Res.*, *104*(31), 697–709.
Grenfell, T. C., S. P. Neshyba, and S. G. Warren (2005), Representation of a nonspherical ice particle by a collection of independent spheres for scattering and absorption of radiation: 3. Hollow columns and plates, *J. Geophys. Res.*, *110*, D17203, doi:10.1029/2005JD005811.
Hadley, O., and W. Kirchstetter (2012), Black-carbon reduction of snow albedo, *Nat. Clim. Change*, *2*(437–440), 2012.
Hisakawa, N., S. D. Quistad, E. R. Hestler, D. Martynova, H. Maughan, E. Sala, M. V. Gavrilo, and F. Rowher (2015), Metagenomic and satellite analyses of red snow in the Russian Arctic, *Peer J*, *3*, e1491, doi:10.7717/peerj.1491.
Hodson, A., H. Paterson, K. Westwood, K. Cameron, and J. Laybourn-Parry (2013), A blue-ice ecosystem on the margins of the East Antarctic ice sheet, *J. Glaciol.*, *59*(214), 255–268.
Hoffer, A., A. Gelencser, P. Guyon, G. Kiss, O. Schmid, G. P. Frank, P. Artaxo, and M. O. Andreae (2006), Optical properties of humic-like substances (HULIS) in biomass-burning aerosols, *Atmos. Chem. Phys.*, *6*, 3563–3570.
Hoham, R. W., and B. Duval (2001), Microbial ecology of snow and freshwater ice with emphasis on snow algae, in *Snow Ecology: An Interdisciplinary Examination of Snow-Covered Ecosystems*, edited by H. G. Jones et al., pp. 168–228, Cambridge Univ. Press, Cambridge.
Holzinger, A., M. C. Allen, and D. D. Deheyn (2016), Hyperspectral imaging of snow algae and green algae from aeroterrestrial habitats, *J. Photochem. Photobiol. B Biol.*, *162*, 412–420, doi:10.1016/j.jphotobiol.2016.07.001.
Irvine-Fynn, T. D. L., A. Edwards, S. Newton, H. Langford, S. M. Rassner, J. Telling, A. M. Anesio, and A. J. Hodson (2012), Microbial cell budgets of an Arctic glacier surface quantified using flow cytometry, *Environ. Microbiol.*, *14*(11), 2998–3012.
Jin, Z., T. P. Charlock, K. Rutledge, K. Stamnes, and Y. Wang (2006), Analytical solution of radiative transfer in the coupled atmosphere–ocean system with a rough surface, *Appl. Optics*, *45*, 7443–7455.
Kandilian, R., E. Lee, and L. Pilon (2013), Radiation and optical properties of *Nannochloropsis oculata* grown under different irradiances and spectra, *Bioresour. Technol.*, *137*(2013), 63–73.
Kokhanovsky, A. A., and E. P. Zege (2004), Scattering optics of snow, *Appl. Optics*, *43*, 1589–1602.
Langford, H., A. Hodson, S. Banwart, and C. Boggild (2010), The microstructure and biogeochemistry of Arctic cryoconite granules, *Ann. Glaciol.*, *51*(56), 87–94.
Laven, P. (2006), MiePlot. [Available at http://www.philiplaven.com/mieplot.htm.]
Lee, F., R.-L. Heng, and L. Pilon (2013), Spectral optical properties of selected photosynthetic microalgae producing biofuels, *J. Quant. Spectros. Radiat. Transfer*, *114*, 122–135, doi:10.1016/j.jqsrt.2012.08.012.
Leya, T. (2004), *Feldstudien und genetische Untersuchungen zur Kryophilie der Schneealgen Nordwestspitzbergens*, Shaker, Aachen.
Li, Y., N. Scales, R. E. Blankenship, R. D. Willows, and M. Chen (2012), Extinction coefficient for red-shifted chlorophylls: Chlorophyll *d* and chlorophyll *f*, *Biochim. Biophys. Acta*, *1817*, 1292–1298.
Libois, Q., G. Picard, J. France, L. Arnaud, M. Dumont, C. Carmagnola, and M. D. King (2013), Influence of grain shape on light penetration in snow, *The Cryosphere*, *7*, 1803–1818, doi:10.5194/tc-7-1803-2013.
Lutz, S., A. M. Anesio, S. E. Jorge Villar, and L. G. Benning (2014), Variations of algal communities cause darkening of a Greenland glacier, *FEMS Microbiol. Ecol.*, *89*, 402–414, doi:10.1111/1574-6941.12351.
Lutz, S., A. M. Anesio, A. Edwards, and L. G. Benning (2015), Microbial diversity on Icelandic glaciers and ice caps, *Front. Microbiol.*, *6*(307), doi:10.3389/fmicb.2015.00307.
Matzl, M., and M. Schneebeli (2006), Measuring specific surface area of snow by near-infrared photography, *J. Glaciol.*, *52*, 558–564.
Minhas, A. K., P. Hodgson, C. J. Barrow, and A. Adholeya (2016), A review on the assessment of stress conditions for simultaneous production of microalgal lipids and carotenoids, *Front. Microbiol.*, *7*, 546, doi:10.3389/fmicb.2016.00546.
Neshyba, S. P., T. C. Grenfell, and S. G. Warren (2003), Representation of a nonspherical ice particle by a collection of independent spheres for scattering and absorption of radiation: 2. Hexagonal columns and plates, *J. Geophys. Res.*, *108*(D15), 4448, doi:10.1029/2002JD003302.
Nicodemus, F. F., J. C. Richmond, J. J. Hsia, I. W. Ginsberg, and T. Limperis (1977), Geometrical considerations and nomenclature for reflectance, *U.S. Department of Commerce Nation al Bureau of Standards, Monograph 160, October 1977*.
Nolin, A. W., and J. Dozier (2000), A hyperspectral method for remotely sensing the grain size of snow, *Remote Sens. Environ.*, *74*, 207–216, doi:10.1016/s0034-4257(00)00111-5.
Painter, T. H., and J. Dozier (2004), Measurements of the hemispherical-directional reflectance of snow at fine spectral and angular resolution, *J. Geophys. Res.*, *109*, D18115, doi:10.1029/2003JD004458.
Painter, T. H., B. Duval, and W. H. Thimas (2001), Detection and quantification of snow algae with an airborne imaging spectrometer, *Appl. Environ. Microbiol.*, *67*(11), 5267–5272, doi:10.1128/AEM.67.11.5267-5272.2001.
Painter, T. H., M. G. Flanner, G. Kaser, B. Marzeion, R. A. VanCuren, and W. Abdalati (2013), End of the Little Ice Age in the Alps forced by industrial black carbon, *Proc. Natl. Acad. Sci. U.S.A.*, *110*(38), 15,216–15,221, doi:10.1073/pnas.1302570110.
Pottier, L., J. Pruvost, J. Deremetz, J.-F. Cornet, J. Legrand, and C. G. Dussap (2005), A fully predictive model for one-dimensional light attenuation by *Chlamydomonas reinhardtii* in a torus photobioreactor, *Biotechnol. Bioeng.*, *91*, 569–582, doi:10.1002/bit.20475.

Quirantes, A., and S. Bernard (2004), Light scattering by marine algae: Two-layer spherical and non-spherical models, *J. Quant. Spectrosc. Radiat. Transfer.*, *89*, 311–321.

Remias, D., U. Lütz-Meindl, and C. Lütz (2005), Photosynthesis, pigments and ultrastructure of the alpine snow alga *Chlamydomonas nivalis*, *Eur. J. Phycol.*, *40*(3), 259–268, doi:10.1080/09670260500202148.

Remias, D., A. Albert, and C. Lutz (2010), Effects of realistically simulated, elevated UV irradiation on photosynthesis and pigment composition of the alpine snow alga *Chlamydomonas nivalis* and the arctic soil alga *Tetracystis* sp. (Chlorophyceae), *Photosynthetica*, *48*(2), 269–277.

Schaepman-Strubb, G., M. E. Schaepman, T. H. Painter, S. Dangel, and J. V. Martonchik (2006), Reflectance quantities in optical remote sensing – definitions and case studies, *Remote Sens. Environ.*, *103*, 27–42.

Slater, J. F., L. A. Currie, J. E. Dibb, and J. B. A. Benner (2002), Distinguishing the relative contribution of fossil fuel and biomass combustion aerosols deposited at Summit, Greenland through isotopic and molecular characterization of insoluble carbon, *Atmos. Environ.*, *36*, 4463–4477.

Stamnes, K., and J. J. Stamnes (2016), Radiative transfer in coupled environmental systems. Wiley VCH Verlag GmbH and co., Weinheim, Germany, 18 March 2016. ISBN: 978-3-527-41138-2.

Stibal, M., J. Elster, M. Sabacka, and K. Kastovska (2007), Seasonal and diel changes in photosynthetic activity of the snow alga *Chlamydomonas nivalis* (*Chlorophycaea*) from Svalbard determined by pulse amplitude modulation fluorometry, *FEMS Microbiol. Ecol.*, *59*, 265–273.

Stramski, D., and A. Morel (1990), Optical properties of photosynthetic picoplankton in different physiological states as affected by growth irradiance, *Deep Sea Res. Part A*, *37*(2), 245–266.

Stramski, D., and D. A. Kiefer (1991), Light scattering by microorganisms in the open ocean, *Prog. Oceanogr.*, *28*, 343–383.

Stramski, D., E. Boss, D. Bogucki, and K. J. Voss (2004), The role of seawater constituents in light backscattering in the ocean, *Prog. Oceanogr.*, *61*, 27–56.

Takeuchi, N., S. Kohshima, and K. Seko (2001), Structure, formation and darkening process of albedo-reducing material (cryoconite) on a Himalayan glacier: A granular algal mat growing on the glacier, Arctic, *Antarct. Alp. Res.*, *33*(2), 115–122.

Takeuchi, N., R. Dial, S. Kohshima, T. Segawa, and J. Uetake (2006), Spatial distribution and abundance of red snow algae on the Harding Icefield, Alaska derived from a satellite image, *Geophys. Res. Lett.*, *33*, L21502, doi:10.1029/2006GL027819.

Thomas, W. H. (1972), Observations on snow algae in California, *J. Phycol.*, *8*(1), 1–9, doi:10.1111/j.1529-8817.1972.tb03994.x.

Uličný, J. (1992), Lorenz-Mie light scattering in cellular biology, *Gen. Physiol. Biophys.*, *11*, 133–151.

Warren, S. G. (1982), Optical properties of snow, *Rev. Geophys.*, *20*(1), 67–89, doi:10.1029/RG020i001p00067.

Warren, S. G., and R. E. Brandt (2008), Optical constants of ice from the ultraviolet to the microwave: A revised compilation, *J. Geophys. Res.*, *113*, D14220, doi:10.1029/2007JD009744.

Warren, S. G. (2013), Can black carbon in snow be detected by remote sensing?, *J. Geophys. Res. Atmos.*, *118*, 779–786, doi:10.1029/2012JD018476.

Waterman, P. C. (1965), Matrix formulation of electromagnetic scattering, *Proc. IEEE*, *53*, 805–812.

Wiscombe, W. J., and S. G. Warren (1980), A model for the spectral albedo of snow. I: Pure snow, *J. Atmos. Sci.*, *37*, 2712–2733, doi:10.1175/1520-0469(1980)0372.0.CO;2.

Xie, Y., P. Yang, B. C. Gao, and M. I. Mischchenko (2006), Effect of ice crystal shape and effective size on snow bidirectional reflectance, *J. Quant. Spectros. Radiat. Transfer*, *100*(1), 457–469, doi:10.1016/j.jqsrt.2005.11.056.

Yamaguchi, S., H. Motoyoshi, T. Tanikawa, T. Aoki, M. Niwano, Y. Takeuchi, and Y. Endo (2014), Application of snow specific surface area measurement using an optical method based on near-infrared reflectance around 900-nm wavelength to wet snow zones in Japan, *Bull. Glaciol. Res.*, *32*, 55–64, doi:10.5331/bgr.32.55.

Zatko, M. C., and S. G. Warren (2015), East Antarctic sea ice in spring: Spectral albedo of snow, nilas, frost flowers and slush, and light absorbing impurities in snow, *Ann. Glaciol.*, *56*(69), 53–64, doi:10.3189/2015AoG69A574.

Zatko, M. C., T. C. Grenfell, B. Alexander, S. J. Doherty, J. L. Thomas, and X. Yang (2013), The influence of snow grain size and impurities on the vertical profiles of actinic flux and associated NO_x emissions on the Antarctic and Greenland Ice Sheets, *Atmos. Chem. Phys.*, *13*, 3547–3567, doi:10.5194/acp-13-3547-2013.